Fluid Structure Interaction (FSI) Study at the Small Bore Connection (SBC) due to Water Hammer

Nur Amalina Binti Mustafa, Prof. Madya Ir. Dr. Nadiahnor Binti Md Yusop

Faculty of Chemical Engineering, Universiti Teknologi MARA

***Abstract*— Water hammer is one of the serious problem that commonly occur in the piping system. Occurrence of this problem can cause physical damage to the pipe and in worst condition, leak will happen and cause burst. The main critical area in this problem is small bore connection which can give negative impact to the structural of pipe. According to definition of water hammer, this problem normally happen when there are changes in fluid velocity caused by sudden closure or opening of pump and valve or electrical failure. In this study, an analysis by using ANSYS Workbench had been done at mainline pipe that have various diameter size of small bore connection. Diameter of small bore connection are varies from 1 inch (25.4 mm) to 2 inch (50.8 mm). The purpose of this study is to find maximum pressure distribution in the pipe. Result shows that maximum pressure distribution inside the pipe is increased when diameter of small bore connection increased for both simulations using different pressure and velocities. Pressure at the point 318 mm from the inlet shows the highest pressure compared to other point. In addition, the study investigated the effect of water hammer on small bore piping by utilizing Finite Element Analysis (FEA). Through this study, the effect that occur on the structure of small bore piping can be expected on certain pressure data. Based on the result if the maximum stress and strain of pipe simulation exceed the maximum stress and strain of carbon steel, small bore piping will deform. From the result analysis that obtained by concluding both objective, it found that the maximum pressure distribution occurred at inlet pressure 4826330 Pa and at inlet velocity 12 m/s at the flange termination. Maximum deformation also occurs at 1 inch small bore connection with these pressure and velocity.**

Keywords*— *Fluid Structure Interaction (FSI), Small Bore Connection, Water Hammer

I. INTRODUCTION

Water Hammer is one of the serious problem that commonly happen in piping system. By definition, water hammer is a pressure transient which will occur due to sudden changes of velocity inside the pipe [1]. Water hammer can also be called as surge pressure or fluid hammer. The term 'water hammer' also can be described as generation, propagation and reflection of pressure waves along pipeline of pressurized liquid system that related with changes in flow condition [2].

Based on the previous study done by Mansuri, Salmasi and Oghati, water hammer can happen in many condition such as sudden closure or opening of the pump or valve and electrical failure [3]. For example, when sudden closure of valve happen, water at the upstream of the valve is continue to flow, creating a vacuum and cause pipe to buckle and crumple. This is because downstream fluid from previously valve tend to continue flowing. In the other hand, when downstream valve closed, mass of fluid before closing the valve will continue flowing forward at uniform velocity. When it hit the closed valve, shock waves will be created. The loud and repetitive bang that can be hear due to closing of valve is coming from shock wave that being travel forward and backward [4].

Occurrence of water hammer in piping system can cause serious problem such as erosion and bending of the pipe. This problem frequently happen in certain condition such as sudden valve closure or opening, sudden pump closure or opening and sudden shut off in piping system due to electrical shortage. Normally, the early sign of water hammer can be seen through the vibration of the pipe and heard the bang sound that comes from inside the pipe.

Besides that, another main area that water hammer always occur is at the junction between mainline pipe and small bore connection. Small bore connection is a branch connection that situated on mainline pipe and designed with diameter less than 2 inch diameter. Types of problem that always happen at small bore connection are fatigue cracking, erosion and corrosion.

Fluid Structure Interaction (FSI) is one of the study that consist of the transfer of momentum and forces between pipe and fluid during unsteady flow condition [5] . Through FSI, the effect of pressure on structural related to few conditions such as deformation, stress and strain can be observed.

In addition, FSI also comprised a few types of coupling such as Poisson Coupling, Friction Coupling and Junction Coupling. Poisson Coupling is a coupling that happened due to radial movement of pipe wall and it caused reduction in fluid speed [6]. This type of coupling also frequently occurred between liquid pressure variation and pipe longitudinal stain. [7]. The generation of axial stress wave can caused it travelled with velocity that have higher propagation of wave than velocity of water hammer and lower speed of sound of pipe [8]. Poisson ratio can also occurred due to radial contraction and expansion of the pipe wall [9]. Friction coupling is happened as the result from wall shear stress. [8]. Wall shear stress can be defined as pressure losses inside fluid equivalent to forces that act on the pipe wall. Friction coupling is occurred between pipe wall and liquid. It is also one of the coupling that occurred when frictional forces are generated between fluid and pipe. When this happen it caused pressure loss in pipe and wall stress changed [9]. When these three effect of coupling are compared, the previous study investigated by Shuaijun Li, Bryan W. Karney and Gongmin Liu found that friction coupling the weakest coupling. Despite of this, in longer period of times, this coupling played an important role for shape and amplitude of wave. [9]. Meanwhile, in term of usage area, Poisson Coupling and Friction Coupling can be used in the entire pipe but for Junction Coupling it can only be used on the junction section such as branch, bend, tees and diameter changes[8].

Therefore, in this studies, it focused on mainline pipe that have small bore connection and small bore piping. This small bore connection might be used as branch connection, drain pipe or refine pipe based on the application of the industry. The investigation involves Fluid Structure Interaction (FSI) modelling on the small bore connection (SBC) that varies in diameter at the range 1 inch (25.4 mm) to 2 inch (50.8 mm). Then maximum pressure of the pipe at the junction between mainline pipe and small bore connection are studied in order to prevent or reduce water hammer effect. Geometry of small bore connection also taken into account when investing the maximum pressure at the junction. The effect of velocity and pressure occurring water hammer on the structure of the small bore connection (SBC) will be discussed in this research studies.

II. METHODOLOGY

A. Physical Method

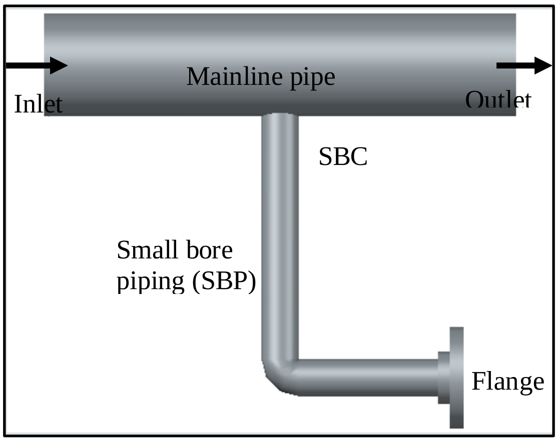

Figure 1: schematic diagram

Figure 1, shown the schematic diagram of this study. The main area of study involved mainline pipe, small bore connection (SBC), small bore piping (SBP) and flange. The measurement for mainline pipe and SBC can be seen in Table 1 and 2.

Table 1: Data for mainline pipe

Diameter , mm	152.4 (6 inch)
Outer diameter (O.D), mm	168.275
Inner diameter (I.D), mm	154.051
Pipe thickness, mm	7.112
Length of pipe, mm	762

The diameter of SBC are varied at 3 different diameters which are 1 inch (25.4 mm), 1.5 inch (38.1 mm) and 2 inch (50.8 mm). The details for each diameter can be seen in Table 2.

Table 2: Data for various diameter of small bore connection (SBC)

Diameter of small bore connection pipe	**25.4 mm (1 inch)**	**38.1 mm (1.5 inch)**	**50.8 mm (2 inch)**
Outer diameter (O.D), mm	33.401	48.26	60.325
Inner diameter (I.D), mm	26.6446	40.894	52.5018
Pipe thickness, mm	3.3782	3.683	3.9116
Length of pipe, mm		674.47	

Grid Independent Study

Grid Independent Study is a study that is done in order to determine the most suitable mesh to be used in study beside reduced the CPU hour. Based on previous study done by W. Pao, L. Hon, A. Saieed, and S. Ban, longer CPU hour are needed to run simulation when mesh is small and number of element is high [10]. Figure 2 showed the grid independence study on the head loss at different velocities versus number of element. Therefore, based on this study, medium mesh is chosen due to suitability and commonly used by other study related to simulation solving by using ANSYS Workbench.

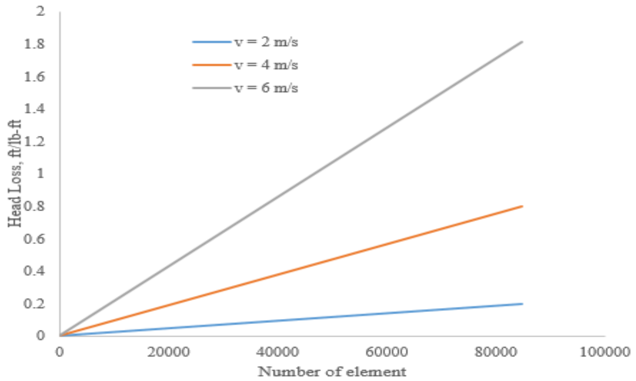

Figure 2: Head loss at different velocity against number of element

B. *Numerical method*

There are three equation that frequently used in order to determine steady and turbulent flow which are continuity, momentum and energy equation.

Continuity equation

Based on the definition, fluid must flow in the way its momentum can be conserved [11]. General equation for incompressible fluid shown in equation 1:

$$\frac{\partial \rho_f}{\partial t} + \frac{\partial(\rho_f v_x)}{\partial x} + \frac{\partial(\rho_f v_y)}{\partial y} + \frac{\partial(\rho_f v_z)}{\partial z} = 0 \quad (1)$$

Where ρ refer to density, t refer to time, ρ_f refer to fluid density and v_x, v_y, v_z are refer to velocity vectors in the x, y and z direction.

Momentum equation

Momentum is define as mass in motion [11]. Equation of momentum can be expressed in equation 2.

$$\frac{\partial(\rho_f v_i)}{\partial t} + v_i\left(\frac{\partial(\rho_f v_x}{\partial x} + \frac{\partial(\rho_f v_y}{\partial y} + \frac{\partial(\rho_f v_z)}{\partial z}\right) = \rho_f g_i - \frac{\partial P}{\partial i} + R_i + \frac{\partial}{\partial x}\left(\mu_e \frac{\partial v_i}{\partial x}\right) + \frac{\partial}{\partial y}\left(\mu_e \frac{\partial v_i}{\partial y}\right) + \frac{\partial}{\partial z}\left(\mu_e \frac{\partial v_i}{\partial z}\right) + T_i \quad (2)$$

Where i refers to x, y and z direction respectively, g_i refers to acceleration, P is fluid pressure, μ_e is effective viscosity. R_i and T_i showed distributed resistance and viscous loss terms respectively.

Energy equation

The equation can be expressed as equation 3 [11].

$$\frac{\partial(\rho_f C_p T)}{\partial t} + \frac{\partial(\rho_f v_x C_p T)}{\partial x} + \frac{\partial(\rho_f v_y C_p T)}{\partial y} + \frac{\partial(\rho_f v_z C_p T)}{\partial z} = \frac{\partial}{\partial x}\left(K\frac{\partial T}{\partial x}\right) + \frac{\partial}{\partial y}\left(K\frac{\partial T}{\partial y}\right) + \frac{\partial}{\partial z}\left(K\frac{\partial T}{\partial z}\right) + Q_v \quad (3)$$

Where C_p is refers to specific heat and T is fluid temperature, v_x, v_y, v_z are amplitudes of velocity vectors in x, y and z direction respectively. Others parameter such as K and Q_V are referred to thermal conductivity and volumetric force respectively.

k-epsilon Model

k-epsilon model is a model that used to describe turbulent flow. There are two equation that represent turbulent flow which are transport equation and turbulent dissipation equation that can be shown in equation 4 and 5 [12]. Table 3 showed the standard value for transport equation and turbulent dissipation equation usage.

$$\frac{\partial}{\partial t}(\rho k) + \frac{\partial}{\partial x_i}(\rho k \mu_i) = \frac{\partial}{\partial x_j}[\left(\mu + \frac{\mu_t}{\sigma_k}\right)\frac{\partial k}{\partial x_j} + \rho k + \rho_b - \rho\varepsilon - Y_k + S_k \quad (4)$$

$$\frac{\partial}{\partial t}(\rho\varepsilon) + \frac{\partial}{\partial x_i}(\rho\varepsilon\mu_i) = \frac{\partial}{\partial x_j}\left[\left(\mu + \frac{\mu_t}{\sigma_\varepsilon}\right)\frac{\partial \varepsilon}{\partial x_j}\right] + C_\varepsilon \frac{\varepsilon}{k}(P_k + C_{3\varepsilon}P_b) - C_{2\varepsilon\rho}\frac{\varepsilon^2}{k} + S_\varepsilon \quad (5)$$

Table 3: Standard data for transport equation and turbulent dissipation equation

σ_k	σ_ε	$\sigma_{1\varepsilon}$	$\sigma_{2\varepsilon}$
1.00	1.30	1.44	1.92

C. Simulation

Finite Volume Method (FVM)

Geometry of fluid domain is created in AUTOCAD and exported to ANSYS Workbench. Boundary condition for this geometry are set at inlet (velocity-inlet), outlet (outflow), wall fluid (wall) and symmetrical (symmetry). In order to solve this solution, k-e model is chosen as it is the most common model to stimulate turbulent flow in Computational Fluid Dynamic (CFD). This study also involved two type of materials which are water (fluid) and carbon steel (solid). Information can be seen in Table 4 and 5.

Table 4: Properties of water

Density, kg/m^3	998
Specific Heat, j/kg-K	4216
Thermal Conductivity, w/m-K	0.677
Viscosity, kg/m-s	0.001003

Table 5: Properties of carbon steel

Density, kg/m^3	7850
Specific Heat, j/kg-K	490
Thermal Conductivity, w/m-K	54

In order to achieve objective of this study, this study are conducted by varied the value of inlet velocity and inlet pressure. Data that used in this simulation can be seen in Table 6 and 7. Data in Table 6 are calculated by using constant the pressure at 3447379 Pa meanwhile for Table 7 is calculated by using constant velocity of fluid at 6 m/s.

Table 6: Data of gauge pressure at different velocity

Velocity, m/s	P_s, Pa	P_g, Pa
3	3442887	3341562
6	3429411	3328086
9	3406952	3305627
12	3375509	3274184

Table 7: Data of gauge pressure at different velocity

Pressure, Pa	P_s, Pa	P_g, Pa
2757903	2739935	2638610
3447379	3429411	3328086
4136854	4118886	4017561
4826330	4808362	4707307

Another parameter that need to be set in this simulation is convergence criteria. There are many type of convergence criteria that can be used in solving the simulation problem. For incompressible fluid, the type of convergence criteria that commonly used is 0.001. The higher the number of convergence criteria, more accurate the result. In this study, absolute convergence criteria is set at 1 x 10^{-5} for all parameters as it is considered as well converged.

Finite Element Method (FEM)

Static structural analysis is an analysis that used to determine stress, strain and deformation that caused by load. Through this analysis, effect of pressure and velocity on structural of small bore connection can be seen through deformation. In this study, carbon steel is used as material for both pipe and blind flange. The density of carbon used is 7850 kg/m^3. For young modulus and Poisson ratio, the value are set at 75 x 10^9 Pa and 0.29 respectively [11].

Medium mesh is used throughout of this study. There are a few parameters that used in order to study the effect on structural which are fixed support and fluid solid interphase. Two fixed support are set on inlet and outlet. This is to prevent the XY plane from moving and effect on the pipe structural can be seen more clearly. Fluid solid interphase is set at the inner part of mainline and branch pipe diameter in order to make sure all the data shared by solid and fluid can be identified in static analysis.

III. RESULTS AND DISCUSSION

A. Finite Volume Method (FVM)

There are five points on the fluid domain had been considered in determination of maximum pressure distribution. The points are set at 0 mm, 181 mm, 381 mm, 581 mm and 762 mm. All of this point are located along the streamline of the fluid. Starting point is set at inlet and end point is set at the outlet. The location of these five points can be observed at Figure 3.

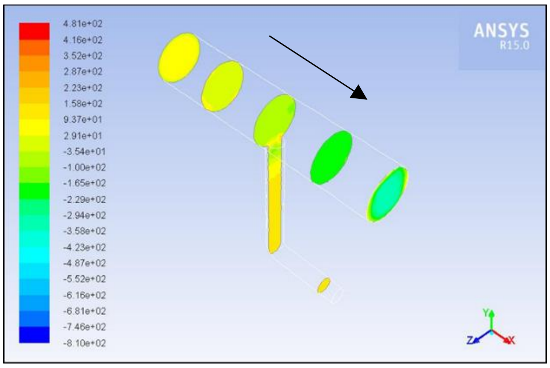

Figure 3: Plane for maximum pressure distribution determination

Pressure distribution at each diameter for different pressure

Figure 4, 5 and 6 is the graphs of pressure distribution at 1 inch diameter, 1.5 inch diameter and 2 inch diameter by varied the inlet pressure of the fluid at 2757903 Pa, 3447379 Pa, 4136854 Pa and 4826330 Pa.

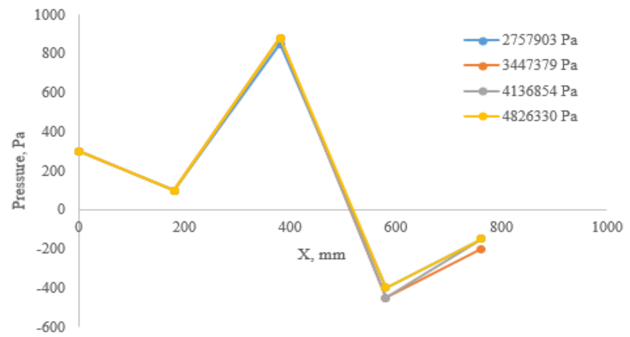

Figure 4: Pressure distribution at 1 inch diameter

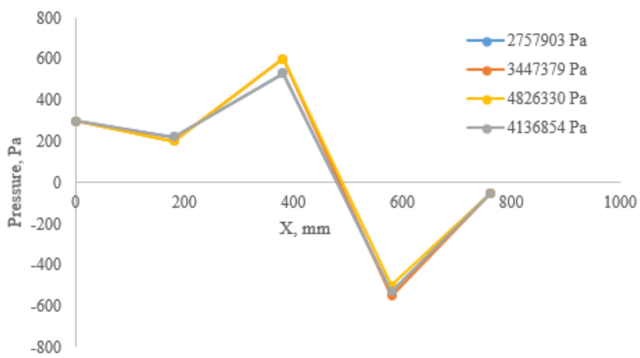

Figure 5: Pressure distribution at 1.5 inch diameter

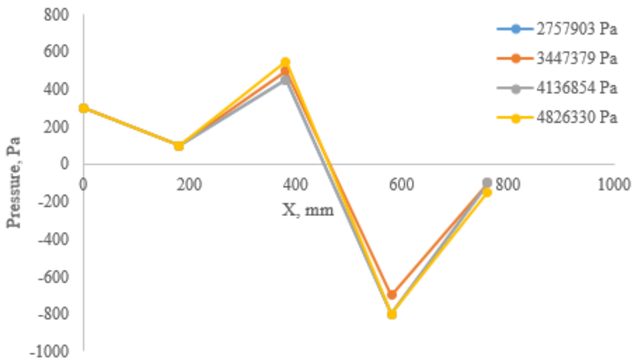

Figure 6: Pressure distribution at 2 inch diameter

Based on Figure 4, 5 and 6, the highest pressure in the fluid can be observed at the point that located 318 mm from the inlet. This point is indicated the junction between mainline pipe and branch pipe. From the graph also, it can be observed that the maximum pressure distribution is occurred at inlet pressure 4826330 Pa for all diameter of small bore connection. This can be proved through previous study from U. Naik and D. Bhat that mentioned, when inlet pressure increases, the maximum pressure distribution will increase [13]. The maximum pressure distribution for different pressure also increase when diameter of small bore connection increase. This is due to large diameter of small bore connection pipe has small surface area that lead to high pressure of fluid inside small bore piping. Therefore, it can be concluded that from this analysis that 1 inch diameter has the highest maximum pressure distribution compared to 1.5 inch and 2 inch diameter of small bore connection.

Pressure Distribution at each diameter for different velocity

Figure 7, 8 and 9, are the graph of pressure distribution at varied velocity which are 3 m/s, 6 m/s, 9 m/s and 12 m/s at different diameter of small bore connection.

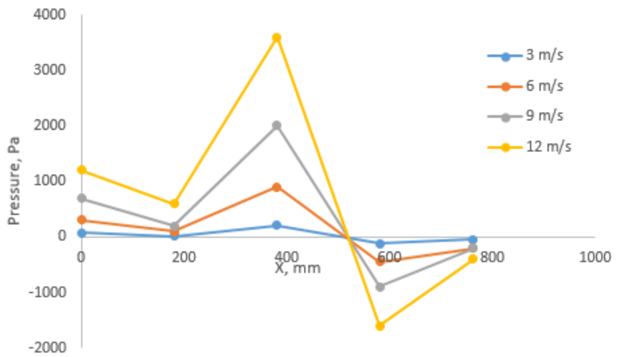

Figure 7: Pressure distribution at 1 inch diameter

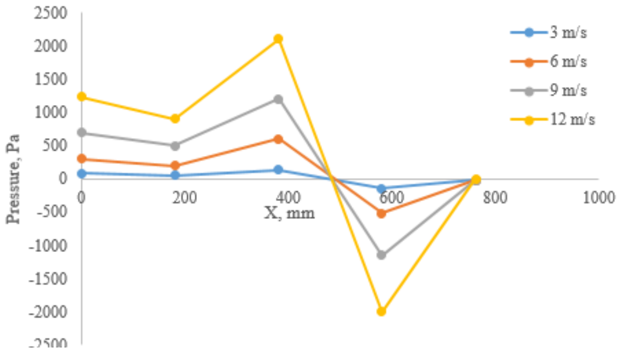

Figure 8: Pressure distribution at 1.5 inch diameter

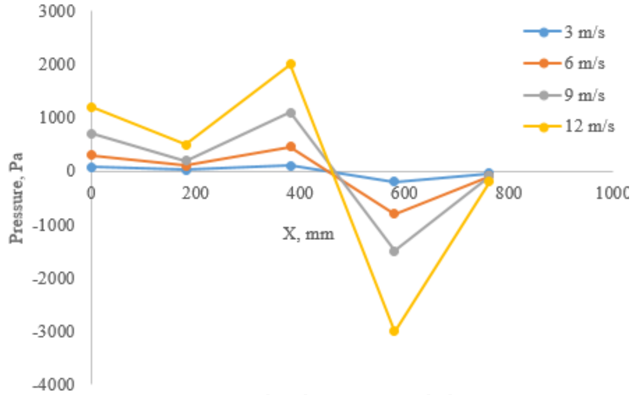

Figure 9: Pressure distribution at 2 inch diameter

Based on the shown in Figure 7, 8 and 9, it can be observed that pressure of fluid at point 318 mm from the inlet is the highest compared to other point because at this is the point where T-junction is located for all three small bore connection. The analysis also shown that when inlet velocity of fluid that flows inside the pipe increase, the maximum pressure distribution also increases. This is because, when fluid in the pipe move faster, the faster the pressure movement forward and backward after hit the wall boundary. Therefore, velocity 12 m/s has the highest maximum pressure distribution. Among these three diameters of small bore connection, it can be observed that maximum pressure distribution at 1 inch diameter is the highest compared to 1.5 inch and 2 inch diameter of small bore connection. This is because based on Bernoulli equation, small diameter has large cross sectional area that lead to high pressure and low velocity. This result proved by statement from Bernoulli equation.

B. Finite Element Method (FEM)

Effect of water hammer on Finite Element Analysis at different pressure

These study are conducted at different pressure. Notation of abject A, B, C and D shown the pressure used in this study.

Notation	Pressure, Pa
A	2757903
B	3447379
C	4136854
D	4826330

Figure 10, 11 and 12 shown the effect of pressure on structural at different diameter of small bore connection.

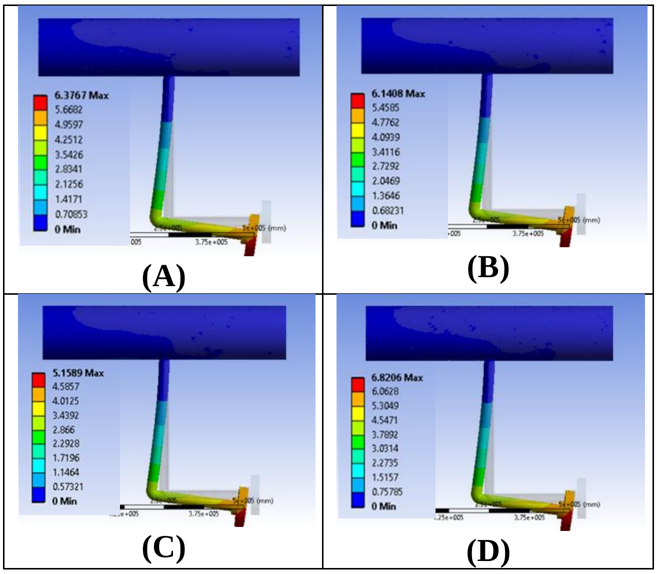

Figure 10: Total deformation at 1 inch diameter

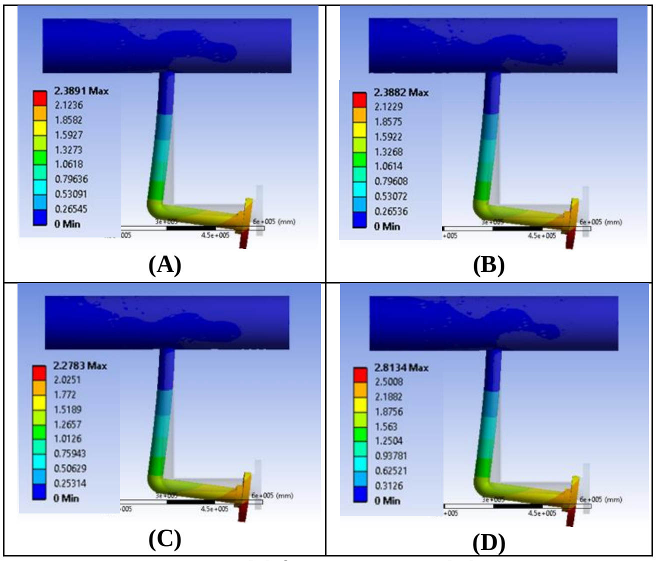

Figure 11: Total deformation at 1.5 inch diameter

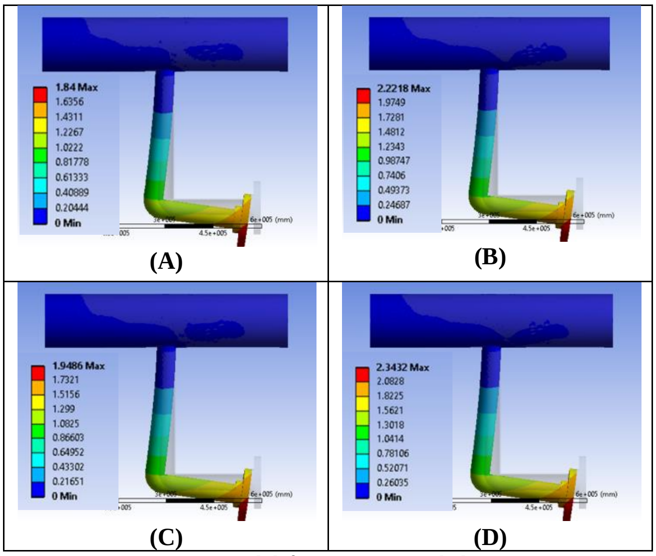

Figure 12: Total deformation at 2 inch diameter

Based on the Figure 8, 9 and 10, it can be observed that when inlet pressure of the fluid increases, total deformation on structural of pipe is decreased until in reach it minimum pressure in pipe. After it reach this minimum value, inlet pressure increased along with the total deformation. In addition, based on figure above, 1 inch diameter of small bore connection has the maximum total deformation compared to other small bore connection. This is because it has small cross sectional area that result in high pressure. This high pressure will continuously hit the wall of pipe until it exceed the maximum strength of pipe material which is carbon steel. Deformation also occur due to another factor such as stress and strain. In this structure, it also been identified that the maximum stress and strain are located at the T-junction that connected between mainline pipe and small bore connection pipe. When the maximum stress and strain of pipe material has been exceed, the pipe will start to deform and in worst condition, pipe can break. Table 11 shown the summary of total deformation at different pressure and diameter. Graph in Figure 13 showed the total deformation of every small bore connection diameter against pressure.

Table 8: Summary data for total deformation at different pressure

Diameter, d (inch)	Total Deformation, mm			
	2757903 Pa	3447379 Pa	4136854 Pa	4826330 Pa
1	6.38	6.14	5.16	6.82
1.5	2.39	2.38	2.28	2.81
2	1.84	2.22	1.95	2.34

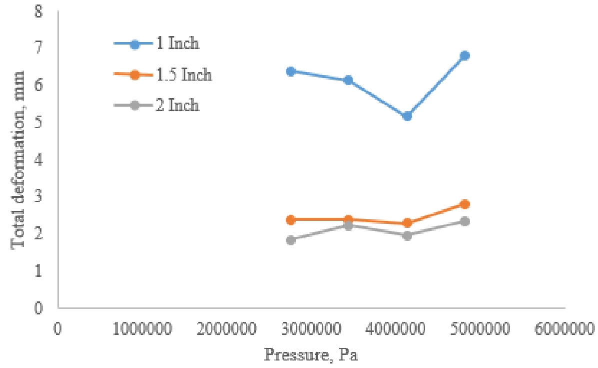

Figure 13: Graph total deformation against pressure

Effect of Finite Element Analysis at different velocities

Velocity of fluid are varied in this study. The notation of abject W, X, Y and Z shown the velocities used in this study.

Notation	Velocities, m/s
W	3
X	6
Y	9
Z	12

Figure 14, 15 and 16 shown the effect of pressure when different velocities are used at different diameter of small bore connection.

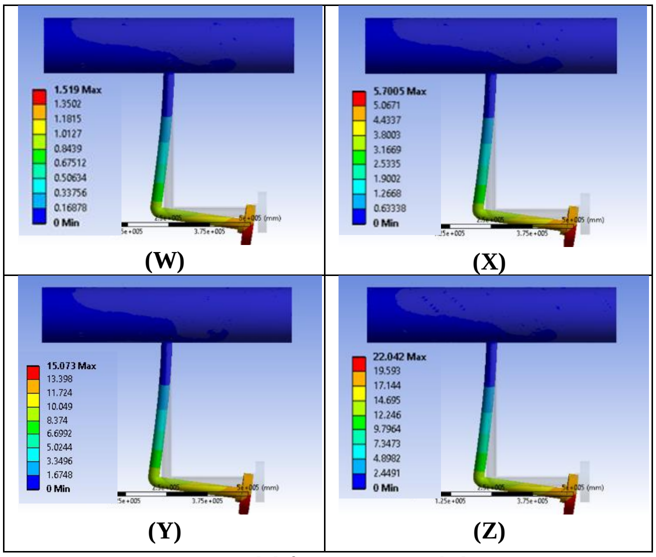

Figure 14: Total deformation at 1 inch diameter

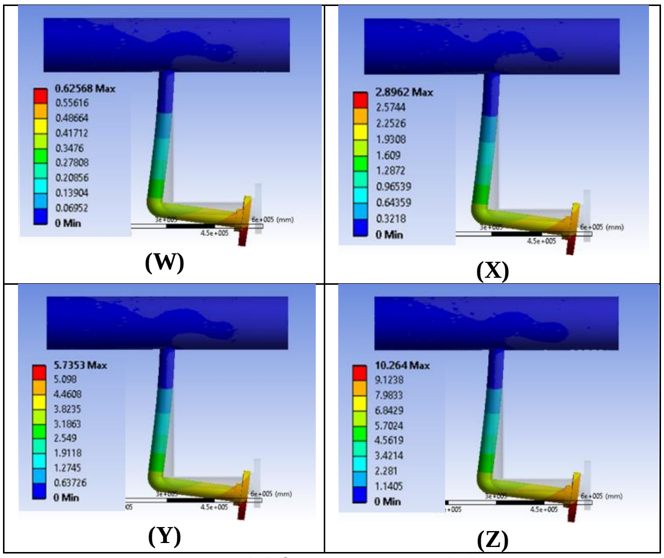

Figure 15: Total deformation at 1.5 inch diameter

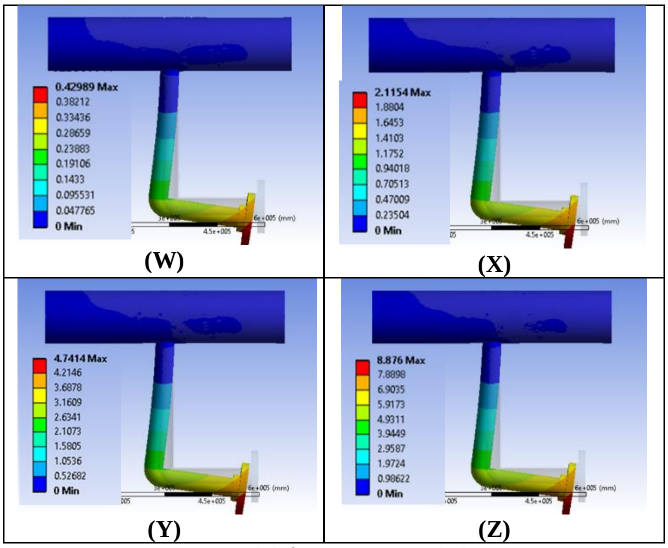

Figure 16: Total deformation at 2 inch diameter

As can be observed from the Figure 14, 15 and 16, maximum total deformation can be seen at 1 inch diameter of small bore connection with velocity 12 m/s. This is because 1 inch diameter has the large cross sectional area that result in high pressure inside the small bore piping. In addition, it can be observed that when inlet velocity of fluid increases, the total deformation also increases. This is because when velocity of the fluid is high, the faster the pressure movement of fluid forward and backward after hit the wall boundary. The summary total deformation for every small bore connection diameter can be observed at Table 15. Graph 17 showed the total deformation of all diameter of small bore connection against velocity of fluid.

Table 15: Summary data of total deformation at different velocities

Diameter, d (inch)	Total deformation, mm			
	3 m/s	6 m/s	9 m/s	12 m/s
1	1.52	5.70	15.07	22.04
1.5	0.63	2.90	5.74	10.26
2	0.43	2.12	4.74	8.88

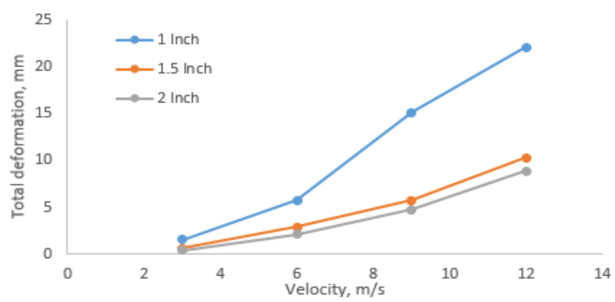

Figure 17: Graph total deformation against pressure

IV. Conclusion

Water hammer is one of the phenomenon that happened due to sudden changes of pressure and velocity at the pump, valve and other related places. This topic has become hot topic among all the industry as it can gave negative impact to the structure. Occurrence of water hammer can caused pipe to bend or corrode especially at small bore connection that has diameter less than 2 inch. Therefore, this study is focused on the Fluid Structure Interaction studies at small bore connection due to water hammer. Based on the result from this simulation, the maximum pressure distribution are obtained at pressure 4826330 Pa and velocity 12 m/s at flange termination. Structure that have 1 inch diameter of small bore connection has the maximum pressure distribution compared to another diameter of small bore connection with these pressure and velocity.

Nomenclature

SBC	Small bore connection
FSI	Fluid Structure Interaction
FVM	Finite Volume Method
FEM	Finite element method
FEA	Finite element analysis
CFD	Computational Fluid Dynamic
ρ	Density, kg/m^3
t	Time, s
ρ_f	Fluid density, kg/m^3
P	Pressure, Pa
μ_e	Effective viscosity, cP
C_p	Specific heat, $J/kg.K$
K	Thermal Conductivity, W/m.K
Q_v	Volumetric force

Acknowledgment

My greatest thank is given to my supervisor, Prof Madya Ir. Dr. Nadiahnor Binti Md Yusop and Universiti Teknologi Mara for giving me advice and guidance in order to complete this study successfully. I also would to give high appreciation to my parent for always giving me motivation and support during these period. Lastly, special thank goes to all my friend, technicians and people who are helping me directly or indirectly during completing this study.

References

[1] S. Lahane, R. Patil, R. Mahajan, and K. Palve, "Analysis of Water Hammering in Pipeline and its CFD Simulation," vol. 3, no. 5, pp. 250–255, 2015.

[2] U. Bulatović and V. Bergant, "Valve-Induced Water Hammer and Column Separation in a Pipeline Apparatus," vol. 60, pp. 742–754, 2014.

[3] B. Mansuri, F. Salmasi, and B. Oghati, "Sensitivity Analysis for Water Hammer Problem in Pipelines," vol. 5, no. 2, pp. 124–131, 2014.

[4] G. Han, K. Ling, N. Dakota, and S. H. Khor, "Simulation of Multiphase Fluid-Hammer Effects During Well Startup and Shut-in," no. December, 2013.

[5] D. C. Wiggert and A. S. Tijsseling, "Fluid transients and fluid-structure interaction in flexible liquid-filled piping," *Appl. Mech. Rev.*, vol. 54, no. 5, p. 455, 2001.

[6] S. Riedelmeier, S. Becker, and E. Schl, "PVP2014-28064," pp. 1–10, 2014.

[7] A. Adamkowski, S. Henclik, W. Janicki, and M. Lewandowski, "European Journal of Mechanics B / Fluids The influence of pipeline supports stiffness onto the water hammer run," vol. 61, pp. 297–303, 2017.

[8] S. Riedelmeier, S. Becker, and E. Schlücker, "Measurements of junction coupling during water hammer in piping systems," *J. Fluids Struct.*, pp. 1–13, 2014.

[9] S. Li, B. W. Karney, and G. Liu, "FSI research in pipeline systems – A review of the literature," *J. Fluids Struct.*, vol. 57, pp. 277–297, 2015.

[10] W. Pao, L. Hon, A. Saieed, and S. Ban, "Numerical simulation of two-phase slug flow with liquid carryover in different diameter ratio T- junction Numerical simulation of two-phase slug flow with liquid carryover in different diameter ratio T-junction," 2017.

[11] X. Li and S. Wang, "Flow field and pressure loss analysis of junction and its structure optimization of aircraft hydraulic pipe system," *Chinese J. Aeronaut.*, vol. 26, no. 4, pp. 1080–1092, 2013.

[12] M. Abdulwahhab, N. K. Injeti, and S. F. D. Dakhil, "Numerical Prediction of Pressure Loss of Fluid in a T-junction," vol. 4, no. 2, pp. 253–264, 2013.

[13] U. Naik and D. . Bhat, "Water Hammering Effects in Pipe System and Dynamic Stress Prediction," *Int. J. Emerg. Res. Manag. Technol.*, vol. 9359, no. 6, pp. 236–243, 2015.